SEMARAK ILMU PUBLISHING

Journal of Advanced Research in Fluid Mechanics and Thermal Sciences

Journal homepage:
https://semarakilmu.com.my/journals/index.php/fluid_mechanics_thermal_sciences/index
ISSN: 2289-7879

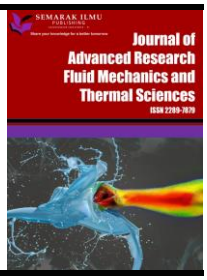

Prediction of Lateral Loads of a Propeller in Oblique Flow by CFD Method

Tran The Nam[1], Nguyen Thi Ngoc Hoa[2], Huynh Van-Vu[3,*]

[1] Vietnam Maritime University, Vietnam
[2] Ho Chi Minh City University of Transport, Vietnam
[3] Nha Trang University, Vietnam

ARTICLE INFO

Article history:
Received 3 July 2024
Received in revised form 18 October 2024
Accepted 1 November 2024
Available online 20 November 2024

Keywords:
Oblique flow; CFD; lateral force; propeller

ABSTRACT

Significant lateral loads on the propeller can be produced under oblique flow conditions, which is critical to the integrity and safety of a ship's stern tube bearing. This paper investigates the effect of oblique flow on lateral loads of a propeller in open water condition based on CFD method. Firstly, the paper provides the theoretical basis for appear the lateral loads of a propeller when working in oblique flow. Then, PPTC propeller was employed as case study. The open water condition is simulated for different inclining angle range of 0 to 12^0. The numerical obtained results indicated that, the lateral loads increase with the oblique flow increasing, and the hydrodynamic forces acted on each propeller blades will be changed over time depending on the relative position of propeller blade as well as the attack angle to the propeller blade. Finally, the paper provides details of flow characteristics around the propeller at different oblique flow angles to explain the change in lateral loads of a propeller when changing the inclining angle.

1. Introduction

Traditionally, marine propellers are designed in the straight flow condition. However, in some cases, the propeller actually operates in the different flow conditions from the design condition such as: propeller installed in the high speed craft with the oblique shaft axis, propeller operating with trim angle, and etc... In those cases, the propellers are definably experienced in the oblique flow condition. Consequently, this oblique flow has not only a significant impact on the propeller efficiency but also inducing a lateral force of the propeller [1-5]. Therefore, it is essentially to conduct a research of determining the lateral force of a propeller due to its presence will directly affect on accurately evaluating the propeller noise, vibration, efficiency, and etc. [6,7].

Currently, thanks to significant advancements in computational resources and numerical methods, the computational fluid dynamics (CFD) method is widely employed to solve the ship hydrodynamics issues in general and propeller performance in particular due to this method shows a huge advantage and has gained popularity in comparison with other method due to it can provide

* *Corresponding author.*
E-mail address: vuhv@ntu.edu.vn

https://doi.org/10.37934/arfmts.124.1.6778

a more physics-based modeling, detail presentation of flow fields, which is very important to study the effect of inclining angle to propeller performance [1-5,8-19]. Currently, there are some studies of lateral force induced by propeller in the oblique flow condition conducted by researchers all over the world. The study of Zhang *et al.,* [16] employing CFD in determining this force in the open water and behind the hull of the ship condition. The results indicated that, the lateral force increases by the increase of oblique angle of the flow in a slightly non-linear trend. Nouroozi and Zeraatgar [1] has evaluated the influence of the oblique flow on the propeller efficiency and the lateral force at the various of oblique angle of flows by CFD methods. The propeller P 4119 was employed as a propeller research model. The authors have conducted a comparison between the research result and those obtained from the straight flow simulations. Guo *et al.,* [2] investigated the hydrodynamic characteristics of a propeller operating in oblique inflow by CFD method. The two propellers with different geometries were employed as the study subjects. The obtained results presented the hydrodynamic mechanism of the propeller operating in oblique inflow. Dubbioso *et al.,* [3] used CFD method to analysis of the performances of a propeller operating in oblique flow. The obtained results provided average and instantaneous loads for both the complete propeller and for a single blade when propeller working in a wide range of incidence angles. Dubbioso *et al.,* [5] conducted analysis effect of oblique flow on marine propeller performance at very high incidence angles by CFD method.

Being inspired of the above problem and base on the heritance of all the previous research results, this paper will present the methodology for appearing the lateral loads of a propeller working in oblique flow and implement the simulation calculation of lateral force induced by propeller working in various oblique flow conditions by CFD method. The discrepancy of flow around the propeller at the various oblique flow angles will be presented and analyzed to provide an intuitively explanation of the nature inducing the change of propeller performance. The propeller Potsdam Propeller Test Case (PPTC) at model-scale was selected to be a researched object.

2. Methodology

Figure 1 demonstrated the analyzing diagram of flow toward the propeller in the oblique flow condition. At the propeller position angle $\theta = 0^0$ (blade number 3), the propeller only has the horizontal flow component. As increasing of position angle in counterclockwise direction to θ_1, the flow reach to the propeller blade is divided into two components including an axial velocity V_x and a circumferential velocity V_t, which are defined in the Eq. (1) and Eq. (2), respectively. When the circumferential position angle continues to increase to θ_2 the magnitude of circular velocity component reduces. Consequently, the lateral force is generated due to the non-uniform distribution of loading on the propeller blades.

$$V_x = U\cos\beta \tag{1}$$

$$V_t = \omega r - U\sin\beta\sin\theta \tag{2}$$

where:
U – is the velocity of the oblique inflow;
ω – is the rotation angular velocity of the propeller;
β – oblique inflow angle (angle between the inflow direction and propeller shaft axis);
θ - is the circumferential position angle of propeller blade.

When the propeller rotates, the oblique flow angle β is constant, the axial velocity component

along propeller shaft V_x and the infinity flow velocity U are constant, and however, the circumferential flow velocity will change with a period of 360 degrees of propeller rotation. In which, the attack angle of flow to the propeller profile will definitely change as the propeller rotates, and it can be estimated by Eq. (3).

$$\alpha = \Phi - \arctan\left(\frac{V_x}{V_t}\right) \tag{3}$$

where: Φ is the pitch angle of a propeller blade.

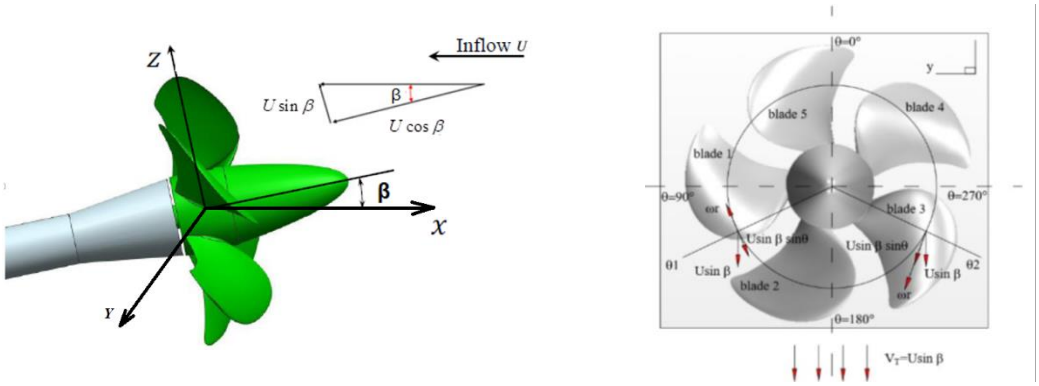

(a) Definition of the blade angle and diagram of the transversal flow

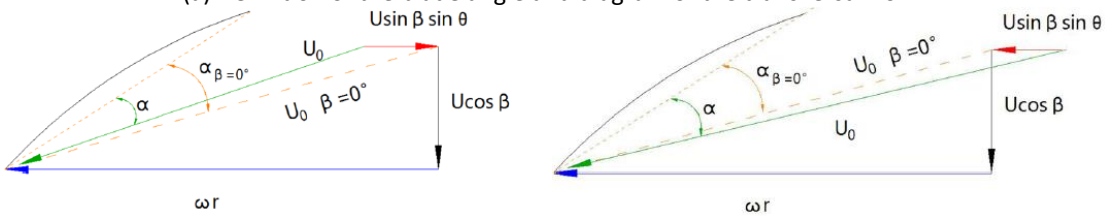

(b) Velocity polygon of Blade 1 (c) Velocity polygon of Blade 3 section

Fig. 1. Hydrodynamic analysis of blade section in oblique flow condition

It can be seen from Eq. (3) that at a higher axial velocity of flow, the higher attack angle values, the thrust increases.

Thus, according to the theoretical basis mentioned above, when the propeller operated in the oblique flow is including six load components on the propeller: 03 force and 03 moment components around the 3 coordinates. To demonstrate these six load components, the following dimensionless coefficients are applied:

$$K_{Tx} = \frac{T_x}{\rho n^2 D^4}, K_{Ty} = \frac{T_y}{\rho n^2 D^4}, K_{Tz} = \frac{T_z}{\rho n^2 D^4}$$
$$K_{Qx} = \frac{Q_x}{\rho n^2 D^5}, Q_{Ty} = \frac{Q_y}{\rho n^2 D^5}, Q_{Tz} = \frac{Q_z}{\rho n^2 D^5} \tag{4}$$

The propeller efficiency is defined as follows:

$$\eta_0 = \frac{K_{Tx}}{K_{Qx}} \times \frac{J}{2\pi} \tag{5}$$

where T_i (T_x, T_y, T_z) and Q_i (Q_X, Q_Y, Q_Z) are force and moment loads on the propeller in the coordinate

axis x, y, z; *n* is the propeller revolution, D is propeller diameter.

The lateral force and moment induced by propeller in this case study are the force in OY direction and moment around 0Y.

3. Numerical Simulation of Lateral Force Induced by Propeller Working in the Oblique Flow

3.1 Propeller Model

In this paper, PPTC propeller was employed as a simulation propeller model. The main characteristics and geometry of the PPTC propeller is depicted in Figure 2 and Table 1 [20,21].

Fig. 2. PPTC propeller

Table 1
The main characteristics of PPTC propeller

Parameter	Symbol	Unit	Value
Diameter of Propeller	D	[m]	0.250
Pitch ratio at 0.75D	P0.75/D	[-]	1.635
Expanded area ratio	A_E/A0	[-]	0.779
Number of blades	Z	[-]	5
Revolution	*n*	[rps]	15.0

3.2 Case Studies

To evaluate the lateral force generated by propeller in oblique flow, this research conducted the simulation for four values of oblique angles: 0^0, 4^0, 8^0, and 12^0 corresponding to 04 variations of advance ratio J=0.8, 1.0, 1.2 and 1.4.

3.3 Simulation Setup

In general, the setup for the CFD computational simulation includes: Defining the computational domain, selecting the boundary conditions, choosing mesh type and generating mesh, selecting physical model and setting up the initial values [17]. To simulate the calculation of the lateral force generated by propeller in oblique flow, due to incoming flow to propeller blades is vary in time, so computational domain should be divided into two zones. One is the cylinder zone surrounding the propeller which is used to simulate the propeller rotation, and the second zone is the rectangular surrounding the whole modelled system which is used to simulate the state of open water. Two zones are connected with each other by interface and sliding mesh technique was used to simulate rotation of propeller. The size of the computational domain and the type of boundary condition are selected as depicted in Figure 3. Both zones of the computational domain is discretized by using unstructured trimmed mesh. The mesh was refined in the regions near the propeller, especially at the parts such

as leading edge, trailing edge of the propeller, where have large curvature change. A denser mesh distribution is implemented along the trajectory of the propeller slipstream's development. Based on taking into account the features of the flow field, the longitudinal orientation of the computational domain and the refinement block is positioned at a specific inclining angle relative to the inflow direction. This ensures that the mesh refinement aligns effectively with the characteristics of the propeller slipstream. Furthermore, for enhanced simulation of the boundary layer, the prism layer was used. Eight layers of prism layer are applied to the surfaces of both blades and the hub. The thickness of the first prism layer is 0.002 mm to keep the non-dimensional normal distance y+ below 5 [17].

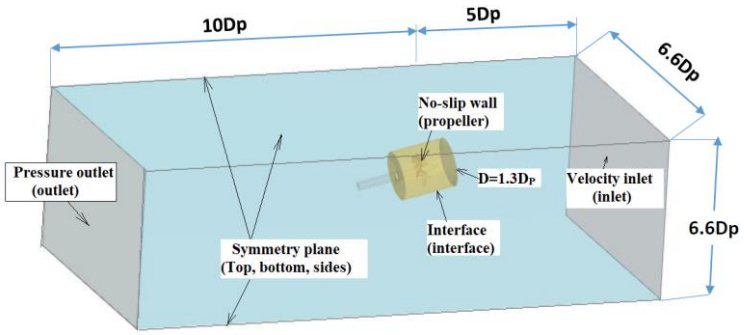

Fig. 3. Computation domain and boundary conditions

The result of mesh generation is presented in Figure 4. The physical model applied in this computation simulation is RANSE method. The turbulence model employed in this paper is SST K-ω model as this model is proved to provide a reliable result and save consuming time in comparison with other turbulence models [8].

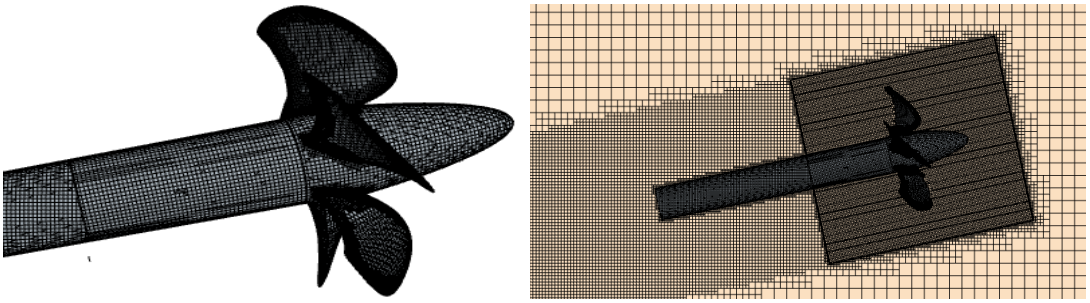

Fig. 4. Mesh generated at oblique angle $\beta=12^0$

4. Simulation Results

4.1 Mesh Convergence Study

A mesh convergence study is conducted to make sure that mesh sizes are sufficient to obtain accurate numerical results. Hence, selecting an appropriate mesh size is of utmost importance for CFD calculations. In this research, the mesh independent verification is performed at advance ratio J = 1.2 and at $\beta=0^0$ and 12^0. The mesh verification results are presented in Table 2. It can be seen in Table 2 that the monotonic convergence was observed for both case studies. Besides, the deviations between CFD results and measured data (EFD) of the thrust (K_{Tx}) and torque (K_{Qx}) coefficients computed for both case studies ($\beta=0^0$ and 12^0) were very small, especially for the fine mesh, the deviations in K_T for both case studies are only 1.36% and 1.98%, respectively, and in K_{Qx} – are 0.90% and 3.10%, respectively. Hence, the fine mesh was applied in further studies.

Table 2
Mesh convergence study at J=1.2 and at β=0^0 and 12^0

Parameters		EFD (D) [20,21]	Mesh solution			ε_{32} %	ε_{21} %	R_G
			Coarse	Medium	Fine			
Straight flow (β = 0^0)								
K_{Tx} [-]	Value	0.295	0.304	0.301	0.299	1.0	0.7	0.67
	E%D	/	3.05	2.03	1.36	/	/	/
$10K_{Qx}$ [-]	Value	0.776	0.789	0.785	0.783	0.510	0.003	0.01
	E%D	/	1.68	1.16	0.90	/	/	/
Oblique flow (β = 12^0)								
K_{Tx} x10^{-3} [-]	Value	0.303	0.314	0.311	0.309	0.965	0.647	0.671
	E%D	/	3.63	2.64	1.98	/	/	/
$10K_Q$ x10^{-3} [-]	Value	0.838	0.871	0.867	0.864	0.461	0.347	0.753
	E%D	/	3.94	3.46	3.10	/	/	/

4.2 Numerical Results of Lateral Force of a Propeller in Oblique Flow

The numerical simulation results of lateral force and moment coefficients generated by propeller working in various oblique flow angles are presented in Table 3 and Figure 5.

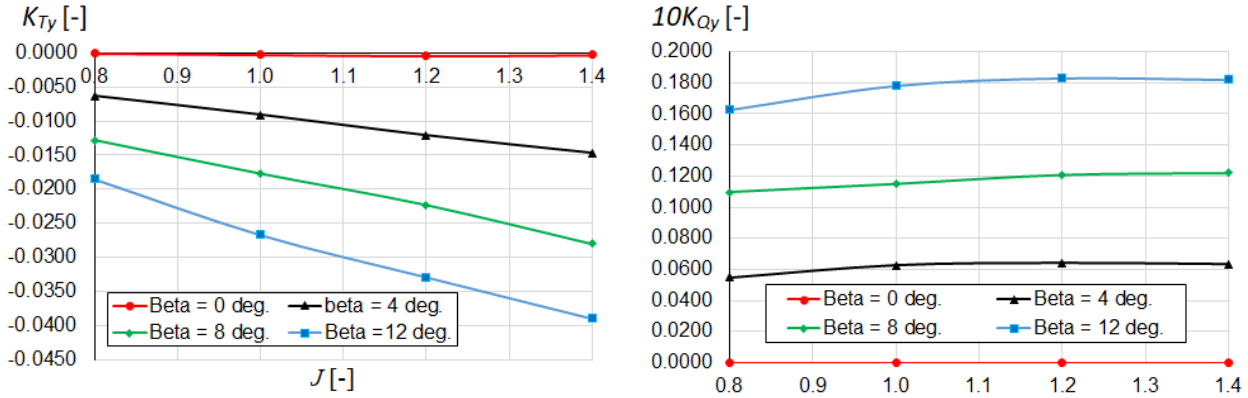

Fig. 5. Lateral hydrodynamic force and moment induced by propeller working in different inflow angles versus J (a) Lateral force and (b) Lateral moment coefficient of propeller

Table 3
Numerical results of lateral force and moment coefficients generated by propeller working in various oblique flow angles

J	Straight flow β=0^0		Oblique flow β=4^0		Oblique flow β=8^0		Oblique flow β=12^0	
	K_{Ty}	$10K_{Qy}$	K_{Ty}	$10K_{Qy}$	K_{Ty}	$10K_{Qy}$	K_{Ty}	$10K_{Qy}$
0.8	0.0001	0.0007	-0.0063	0.0550	-0.0128	0.1095	-0.0185	0.1625
1.0	0.0002	0.0008	-0.0091	0.0625	-0.0177	0.1150	-0.0267	0.1781
1.2	0.0001	0.0009	-0.0121	0.0639	-0.0223	0.1210	-0.0329	0.1830
1.4	0.0002	0.0008	-0.0147	0.0602	-0.0280	0.1222	-0.0390	0.1820

Regarding to the numerically obtained results provided in Table 3 and Figure 5, it can be concluded that:

i. At an advance ratio J, the lateral force (K_{Ty}) and moment coefficients (K_{Qy}) are increased as increasing oblique flow angle and vice versa.
ii. At a constant oblique flow angle (β=constant), an increase of advance ratio (J) lead to an increase of the lateral thrust coefficient (K_{Ty}) and vice versa, however, lateral moment coefficient (K_{Qy}) witnessed a slightly change.

As mentioned in section 2, when the propeller working in the oblique flow the hydrodynamic forces acted on each propeller blades will be changed over time depending on the relative position of propeller blade as well as the attack angle to the propeller blade. Figure 6 depicts the fluctuation and the variation over time of lateral force on each propeller blades. As can be seen in Figure 6, the lateral force induced by propeller changes periodically and its period is the rotational period of the propeller. Moreover, Figure 7 provides the distinct in phase and amplitude of lateral forces induced by one blade in various oblique flow angles of the propeller. The amplitude of lateral forces on each blade monotonically increases when oblique flow angles increase. At $\beta=0^0$, the amplitude of lateral forces ranges from -50.6N to 50.5N, at $\beta=4^0$ it ranges from -54.35N to 48.58N, at $\beta=8^0$ it ranges from -58.2N to 47.65N and at $\beta=12^0$ it ranges from -63.47 to 48.24N. This can be explained by the differences in pressure distribution on each blade surfaces (referred Figure 9).

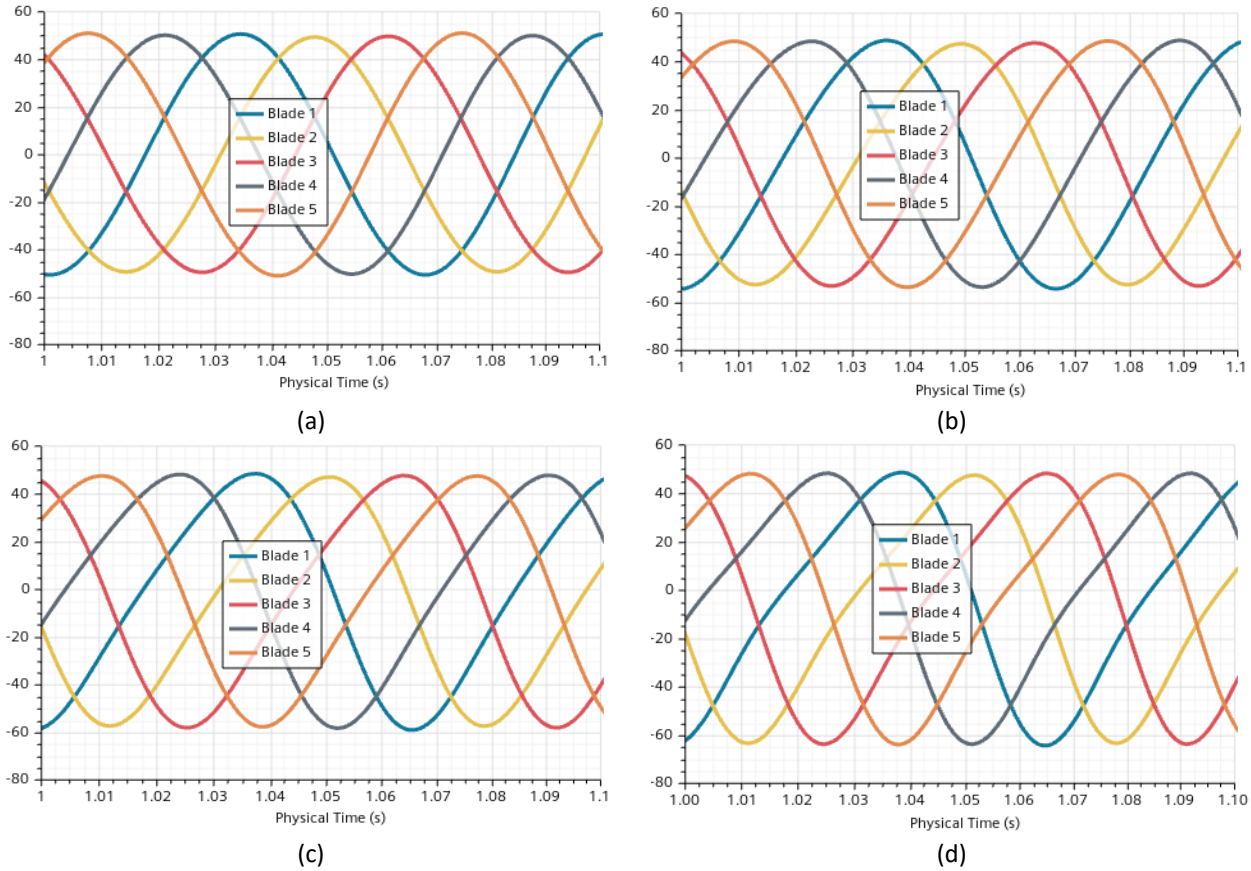

Fig. 6. The change of lateral force on each propeller blade over time in various oblique angles at J=1.0; Oblique beta = (a) 0^0, (b) 4^0, (c) 8^0, (d) 12^0

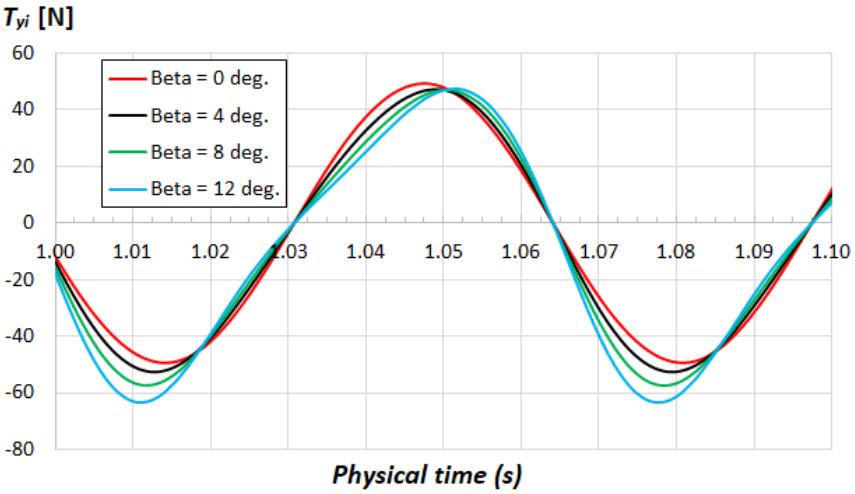

Fig. 7. The change of amplitude and phase of lateral force on blade 2 in various oblique angles at J=1.0

4.3 Effect of Oblique Flow on Flow Around the Propeller

4.3.1 Axial velocity field

Figure 8 shows the axial velocity pattern on Y=0 plane at J=1.4 in various oblique angles. It is clear in Figure 8 that, for straight flow ($\beta=0^0$), the axial velocity pattern is almost axisymmetric, for inclined flow conditions, the axial velocity pattern is asymmetric and the level of its asymmetric increases when increasing inclining angle. Asymmetric in axial velocity pattern is biggest at $\beta=12^0$.

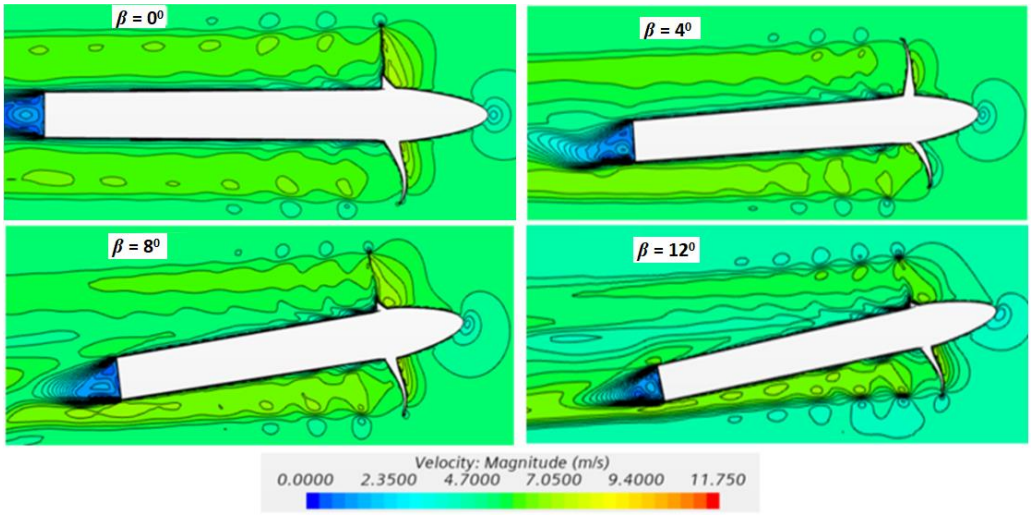

Fig. 8. Axial velocity pattern at J=1.4 in various oblique angles

4.3.2 Pressure distribution

The pressure distribution on suction and pressure sides of the propeller blades under straight and oblique inflow conditions is presented in Figure 9. It can be seen in Figure 9 that, the pressure distribution on the propeller blades change in the circumferential position and its level changes are different inclined flow conditions. The pressure distribution on the propeller blades change in the circumferential position are smallest and biggest at $\beta=0^0$ and $\beta=12^0$, respectively. On the other hand, it can be seen in Figure 9 that, the propeller blades experience a load in the first and second quadrants of the propeller disk (i.e., $0°<\theta<180°$), referred to as the "downwind zone," where the tangential

velocity of the blades aligns with the lateral inflow. Conversely, in the third and fourth quadrants (i.e., 180°<θ<360°), known as the "upwind zone," the blades encounter a significantly higher load as the tangential velocity opposes the lateral inflow. The resulting changes in the pressure distribution on the propeller blades at different oblique angles provide some explanation for changes lateral force generated by propeller.

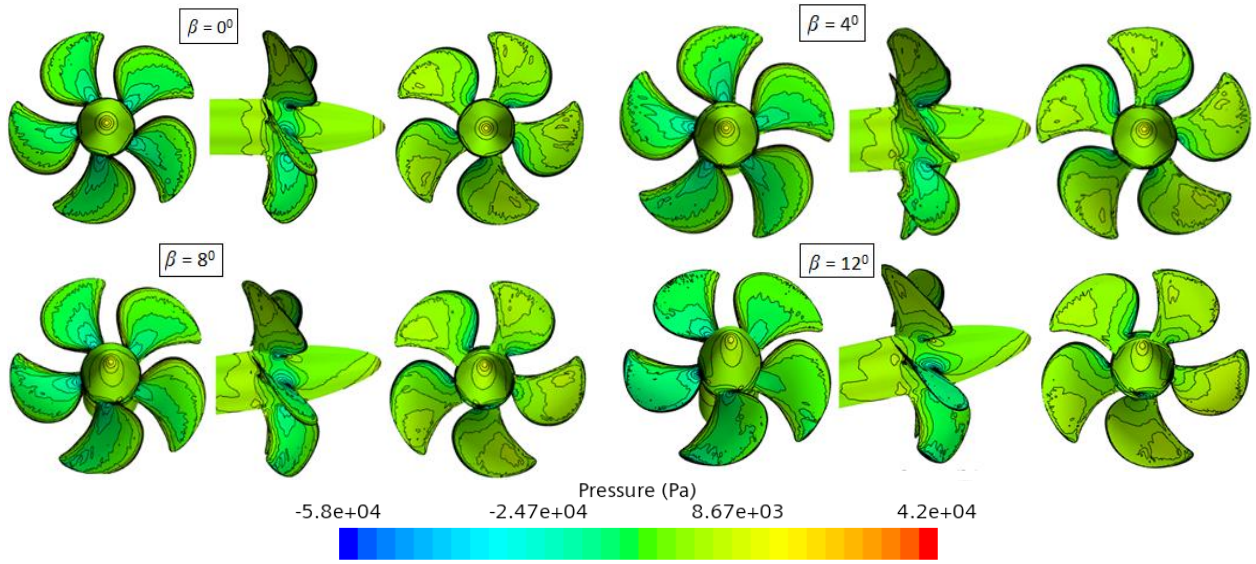

Fig. 9. Pressure distribution on suction and pressure sides of the propeller blades at J=1.4 in various oblique angles

4.3.3 Skin friction coefficient

The skin friction coefficient distribution on suction and pressure sides of the propeller blades under straight and oblique inflow conditions is showed in Figure 10. It can be observed in Figure 10 the tendency and level changes of the skin friction coefficient distribution on propeller blades under different inclined flow conditions are the same as pressure distribution.

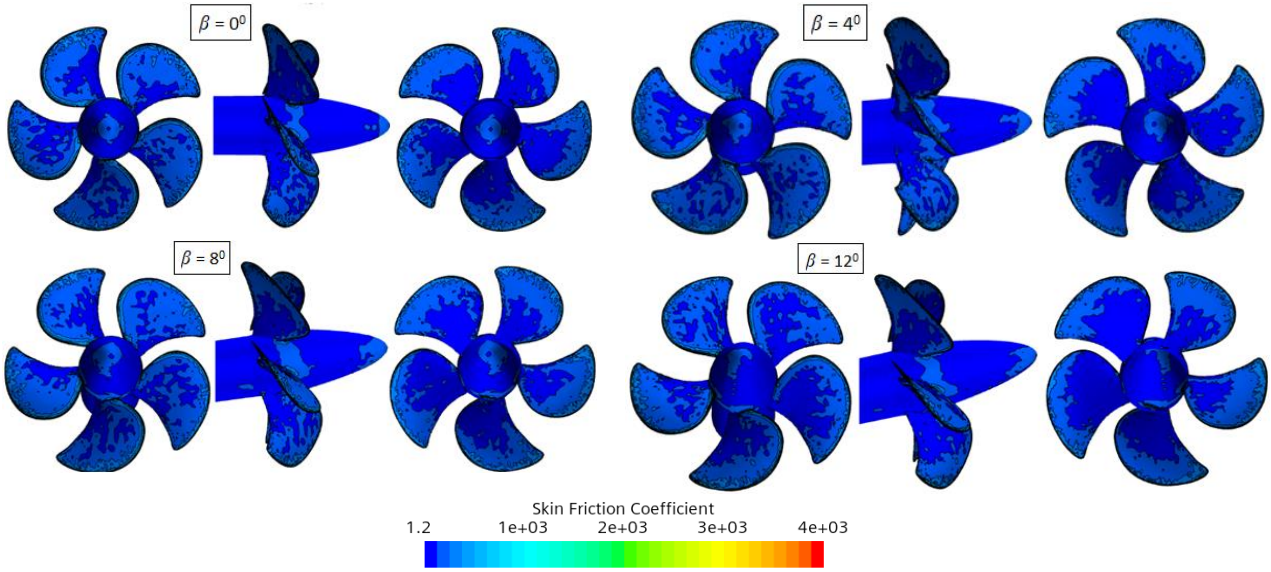

Fig. 10. Skin friction coefficient distribution on suction and pressure sides of the propeller blades at J=1.4 in various oblique angles

4.3.4 Vortices in the wake of the propeller

Vortices in the wake of the propeller is a physical phenomenon of great interest to be investigated, it is recognized to have significantly effect on propeller characteristics. Figure 11 shows the vortices in the wake of the propeller at J=1.4 in various oblique angles. For the case straight inflow conditions ($\beta=0^0$), the propeller slipstream is identified by noticeable tip and hub vortices, and both of them is circumferentially uniform through the axial axis. For the cases with inclined flow conditions, the tip and hub vortices are dynamic change with the circumferential position. The vortex system intensifies at circumferential positions between 180° and 360°, indicating a potential for further development. Conversely, it disperses noticeably between 0° and 180°. As the incidence angle increases, the trajectory of the shedding vortices shifts towards the direction of the lateral inflow.

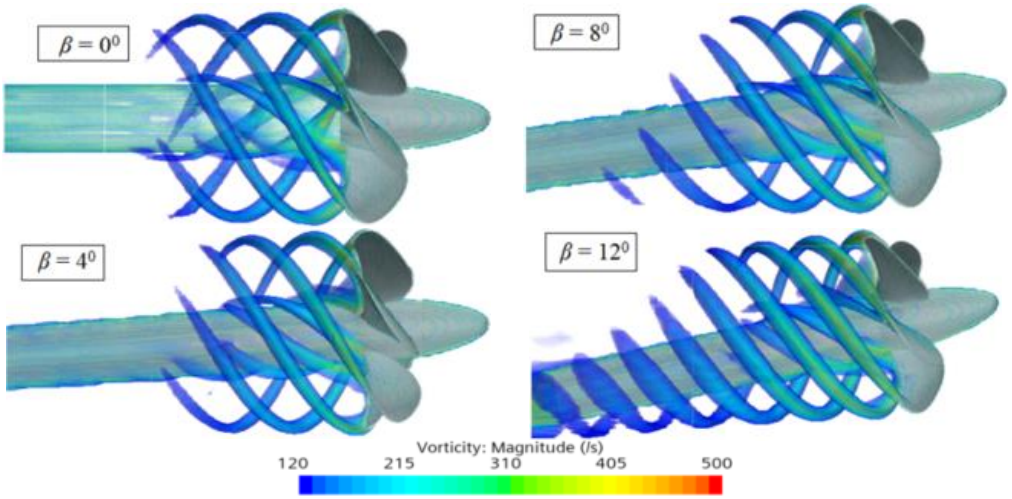

Fig. 11. Vortices in the wake of the propeller at J=1.4 in various oblique angles

5. Conclusions

In this research, CFD method is used to prediction of lateral force generated by propeller operating under oblique inflow conditions. The PPTC propeller at model-scale was selected as the subject study. The simulation is carried out for the propeller working in a wide range of advance ratio and inclining angles. The numerical obtained results have been verified and validated with measured data at a straight inflow ($\beta=0^0$) and inflow angle ($\beta=12^0$) conditions. From the case studies, the following conclusions can be made as follows:

i. Lateral force and moment are generated by propeller at non-zero inflow angles. Increasing the oblique flow angle led to increase the lateral force (K_{Ty}) and moment coefficients (K_{Qy}). The impact of oblique flow on lateral thrust coefficient is more remarkable at high advance coefficients, while on lateral moment coefficient is unpronounced.
ii. The hydrodynamic forces acted on each propeller blades will be changed over time depending on the relative position of propeller blade as well as the attack angle to the propeller blade.

Acknowledgement
The author is grateful to the Vietnam Maritime University and Ho Chi Minh City University of Transport for providing necessary research facilities during current research work. This research was unfunded by any grant.

References

[1] Nouroozi, Hossein, and Hamid Zeraatgar. "Propeller hydrodynamic characteristics in oblique flow by unsteady RANSE solver." *Polish Maritime Research* 1 (2020): 6-17. https://doi.org/10.2478/pomr-2020-0001

[2] Guo, Hai-peng, Zao-jian Zou, Feng Wang, and Yi Liu. "Numerical investigation on the hydrodynamic characteristics of a marine propeller operating in oblique inflow." *Applied Ocean Research* 93 (2019): 101969. https://doi.org/10.1016/j.apor.2019.101969

[3] Dubbioso, Giulio, Roberto Muscari, and Andrea Di Mascio. "Analysis of the performances of a marine propeller operating in oblique flow." *Computers & Fluids* 75 (2013): 86-102. https://doi.org/10.1016/j.compfluid.2013.01.017

[4] Shamsi, Reza, and Hassan Ghassemi. "Determining the hydrodynamic loads of the marine propeller forces in oblique flow and off-design condition." *Iranian Journal of Science and Technology, Transactions of Mechanical Engineering* 41 (2017): 121-127. https://doi.org/10.1007/s40997-016-0049-x

[5] Dubbioso, G., R. Muscari, and A. Di Mascio. "Analysis of a marine propeller operating in oblique flow. Part 2: very high incidence angles." *Computers & Fluids* 92 (2014): 56-81. https://doi.org/10.1016/j.compfluid.2013.11.032

[6] Viviani, Michele, C. Podenzana Bonvino, Salvatore Mauro, Marco Cerruti, D. Guadalupi, and A. Menna. "Analysis of asymmetrical shaft power increase during tight manoeuvres." In *9th International Conference on Fast Sea Transportation (FAST2007)*, Shanghai, China. 2007.

[7] Coraddu, A., G. Dubbioso, S. Mauro, and M. Viviani. "Analysis of twin screw ships' asymmetric propeller behaviour by means of free running model tests." *Ocean Engineering* 68 (2013): 47-64. https://doi.org/10.1016/j.oceaneng.2013.04.013

[8] Ariana, I Made, Riyan Bagus Prihandanu, Dhimas Widhi Handani, and A. A. B. Dinariyana. "Investigation of the Effects of the Pre-Duct in a Ship on Propeller-Hull Interactions Using the CFD Method." *CFD Letters* 15, no. 4 (2023): 17-30. https://doi.org/10.37934/cfdl.15.4.1730

[9] Nasirudin, Ahmad, I Ketut Aria Pria Utama, Sutiyo Sutiyo, and Andreas Kukuh Priyasambada. "CFD Analysis into the Resistance Estimation of Hard-Chine Monohull using Conventional against Inverted Bows." *CFD Letters* 15, no. 6 (2023): 54-64. https://doi.org/10.37934/cfdl.15.6.5464

[10] Tu, Tran Ngoc, Do Duc Luu, Nguyen Thi Hai Ha, Nguyen Thi Thu Quynh, and Nguyen Minh Vu. "Numerical prediction of propeller-hull interaction characteristics using RANS method." *Polish Maritime Research* 2 (2019): 163-172. https://doi.org/10.2478/pomr-2019-0036

[11] Jasak, Hrvoje, Vuko Vukčević, Inno Gatin, and Igor Lalović. "CFD validation and grid sensitivity studies of full scale ship self propulsion." *International Journal of Naval Architecture and Ocean Engineering* 11, no. 1 (2019): 33-43. https://doi.org/10.1016/j.ijnaoe.2017.12.004

[12] Le, Tat-Hien, and Tran Van Tao. "Numerical Investigation of the Scale Effect on the Flow around the Ship by using RANSE Method." *CFD Letters* 15, no. 11 (2023): 67-78. https://doi.org/10.37934/cfdl.15.11.6778

[13] Tu, T. N., N. T. H. Phuong, V. Tuan Anh, V. M. Ngoc, P. T. T. Hai, and C. H. Chinh. "Numerical prediction of ship resistance in calm water by using RANS method." *Journal of Engineering and Applied Sciences* 13, no. 17 (2018): 7210-7214.

[14] Luu, Do Duc, Tran Ngoc Tu, Tran Khanh Toan, Tat-Hien Le, Nguyen Duy Anh, and Nguyen Thi Hai Ha. "Numerical study on the influence of longitudinal position of centre of buoyancy on ship resistance using RANSE method." *Naval Engineers Journal* 132, no. 4 (2020): 151-160.

[15] Le, Tat-Hien, Nguyen Duy Anh, Tran Ngoc Tu, Nguyen Thi Ngoc Hoa, and Vu Minh Ngoc. "Numerical investigation of length to beam ratio effects on ship resistance using RANSE method." *Polish Maritime Research* 30, no. 1 (2023): 13-24. https://doi.org/10.2478/pomr-2023-0002

[16] Zhang, Yu-xin, Kang Chen, and Da-peng Jiang. "CFD analysis of the lateral loads of a propeller in oblique flow." *Ocean Engineering* 202 (2020): 107153. https://doi.org/10.1016/j.oceaneng.2020.107153

[17] Tu, Tran Ngoc. "Numerical simulation of propeller open water characteristics using RANSE method." *Alexandria Engineering Journal* 58, no. 2 (2019): 531-537. https://doi.org/10.1016/j.aej.2019.05.005

[18] Tu, Tran Ngoc, and Nguyen Manh Chien. "comparison of different approaches for calculation of propeller open water characteristic using RANSE method." *Naval Engineers Journal* 130, no. 1 (2018): 105-111.

[19] Adietya, Berlian Arswendo, I Ketut Aria Pria Utama, Wasis Dwi Aryawan, Mochammad Nasir, Nurcholis Nurcholis, Mahendra Indiaryanto, Nurwidhi Asrowibowo, Rizqi Dian Permana, and Nurhadi Nurhadi. "Numerical and Experimental Investigations into the Characteristics of Wageningen B4-70 Series of Propeller with Boss Cap Fins." *CFD Letters* 15, no. 10 (2023): 152-169. https://doi.org/10.37934/cfdl.15.10.152169

[20] Morgut, Mitja, Enrico Nobile, Dragica Jošt, and Aljaž Škerlavaj. "Numerical predictions of the PPTC model propeller in oblique flow." In *Proceedings of the Second Workshop on Cavitation and Propeller Performance, The Fourth*

International Symposium on Marine Propulsors, smp'15, pp. 138-142. Ocean Engineering Group, The University of Texas at Austin and SVA Potsdam GmbH, 2015.

[21] Schiffbau-Versuchsanstalt Potsdam (SVA). "ITTC Benchmarking Test Case." *SVA*, 2023. https://www.sva-potsdam.de/en/ittc-benchmark/.